

1 Accommodating heteroscedasticity in allometric biomass models

2

3 Ioan Dutcă^{1,2,*}, Ronald E. McRoberts³, Erik Næsset⁴, Viorel N.B. Blujdea⁵

4

5 ¹ Department of Silviculture, Transilvania University of Brasov, 1 Şirul Beethoven, Braşov 500123, Romania

6 ² Department of Sustainability, Buckinghamshire New University, Queen Alexandra Rd, High Wycombe HP11 2JZ, UK

7 ³ Department of Forest Resources, University of Minnesota, Saint Paul, MN, United States

8 ⁴ Department of Ecology and Natural Resource Management, Norwegian University of Life Sciences, P.O. Box 5003, 1432

9 Ås, Norway

10 ⁵ Bio-Economy Unit, European Commission Joint Research Centre, Ispra, Italy

11 * Corresponding author. Email address: idutca@unitbv.ro

12

13 Abstract

14 Allometric models are commonly used to predict forest biomass. These models typically take
15 nonlinear power-law forms that predict individual tree aboveground biomass (AGB) as functions of
16 diameter at breast height (D) and/or tree height (H). Because the residual variance is in most cases
17 heteroscedastic, accommodating the heteroscedasticity (i.e., heterogeneity of variance) becomes
18 necessary when estimating model parameters. We tested several weighting procedures and a
19 logarithmic transformation for nonlinear allometric biomass models. We further evaluated the
20 effectiveness of these procedures with emphasis on how they affected estimates of mean AGB per
21 hectare and their standard errors for large forest areas. Our results revealed that some weighting
22 procedures were more effective for accommodating heteroscedasticity than others and that
23 effectiveness was greater for single predictor models but less for models based on both D and H.
24 Failing to effectively accommodate heteroscedasticity produced small to moderate differences in the
25 estimates of mean AGB per hectare and their standard errors. However, these differences were greater
26 between model forms (models based on D and H versus models based on D only), regardless of the
27 weighting approach. Similar consequences were observed with respect to whether model prediction
28 uncertainty was or was not included when estimating mean AGB per hectare and standard errors.
29 When including model prediction uncertainty, the standard errors of the estimated means increased

30 substantially, by 44-59%. Therefore, to avoid possible negative consequences on large-area biomass
31 estimation, we recommend three steps: (i) testing the effectiveness of a weighting procedure when
32 accommodating heteroscedasticity in allometric biomass models, (ii) incorporating model prediction
33 uncertainty in the total uncertainty estimate and (iii) including H as an additional predictor variable in
34 allometric biomass models.

35

36 **Keywords:** aboveground biomass, allometric model, weighted regression, error propagation,
37 homoscedasticity.

38 1. Introduction

39 The accuracy and precision of forest biomass estimates play a critical role for the relevance of forests
40 within the climate change mitigation framework (Bonan, 2008; Canadell and Raupach, 2008; Grassi
41 et al., 2017; Pan et al., 2011). Large area forest biomass estimates typically rely on individual tree
42 allometric models constructed using individual tree measurements of aboveground biomass (AGB,
43 kg), diameter at breast height (D, cm) and tree height (H, m) for a sample of trees, hereafter
44 designated the *calibration sample*. Ideally, these trees should be selected from the same population as
45 the population to which the models will be applied, but in practice they are often at least partially
46 selected from outside the population of interest (McRoberts et al., 2016). The models are applied
47 using measurements of a set of individual tree D and H for all trees on a second sample of plots,
48 hereafter designated the *inventory sample*.

49 By combining the information from the calibration and the inventory samples, the aim is to
50 develop an estimator of mean biomass per hectare for the population of interest which is then
51 converted to carbon estimates using a biomass to carbon conversion factor. Often, the uncertainty
52 associated with the allometric biomass model predictions is ignored with only the sampling variability
53 (i.e., plot-to-plot variability) associated with the probability-based (design-based) estimator reported.
54 In some circumstances, this practice is justified by the insignificant levels of uncertainty associated
55 with the allometric model predictions relative to the sampling variability (McRoberts et al., 2016,
56 2015; McRoberts and Westfall, 2014). To incorporate the allometric model prediction uncertainty
57 and/or other sources of uncertainty, a “hybrid inference” approach can be used (Condés and
58 McRoberts, 2017; Corona et al., 2014; McRoberts et al., 2019, 2016; Ståhl et al., 2016) to produce
59 more accurate estimates of uncertainty.

60 Allometric biomass models are often in the form of nonlinear regression models with the
61 power model being particularly popular:

$$62 \quad AGB_i = \beta_0 \cdot X_i^{\beta_1} + \varepsilon_i \quad (1)$$

63 where AGB_i is aboveground biomass of the i^{th} tree, X_i is a biomass predictor and ε_i is a random
64 residual term. Diameter at breast height (D) is commonly used as predictor of tree AGB, being used

65 frequently as the sole predictor (Chave et al., 2005; Forrester et al., 2017; Luo et al., 2020; Picard et
66 al., 2012; Zianis et al., 2005; Zianis and Mencuccini, 2004), or in combination with tree height (H)
67 (Picard et al., 2015, 2012; Zianis et al., 2005). To explain the effects of interspecific variability, wood
68 density may be added as a third predictor variable, especially for the tropical forests (Chave et al.,
69 2014, 2005; Vieilledent et al., 2012). Compared to simple allometric biomass models that use only D
70 as predictor of AGB, including H has improved the fit of the models (Dutcă, 2019; Rutishauser et al.,
71 2013). Although H can be included in the form of D^2H , Dutcă et al. (2019) suggested that using D and
72 H as distinct predictor variables should be preferred.

73 To ascertain the biological meaning of the scaling exponent β_1 in Eq. (1), Huxley (1932),
74 introduced logarithmic transformations of both response and predictor variables as a way to express
75 the model. Because the residuals associated with allometric biomass model predictions often exhibit
76 heteroscedasticity (i.e. heterogeneity of variance, showing an increase in residual variances with
77 increases in predicted values), logarithmic transformations have been promoted as a way to stabilize
78 the variance, a technique that is widely used nowadays as the default method for fitting allometric
79 models (Asrat et al., 2020; Dutcă et al., 2020, 2018; Luo et al., 2020). With logarithmic
80 transformation, the objective is to obtain a model that has homoscedastic (or relatively
81 homoscedastic) residuals. An advantageous by-product of the transformation is that the model is often
82 linearized which facilitates fitting the model using simpler linear regression rather than nonlinear
83 regression methods. Yet, achieving homoscedasticity and an accurate linear model on the transformed
84 scale is not guaranteed by a ln-ln transformation, thereby leading to an intense debate as to whether
85 logarithmic transformations should or should not be used as the default fitting method (Kerkhoff and
86 Enquist, 2009; Packard, 2014; Packard and Boardman, 2008; Xiao et al., 2011). Nevertheless, the
87 increase in computational power and the widespread availability of nonlinear regression routines in
88 statistical software packages in the last decades has greatly facilitated fitting the models directly in
89 their original untransformed nonlinear forms, thereby avoiding back-transformation correction factors
90 (Baskerville, 1972; Goldberger, 1968; Sprugel, 1983). On the original untransformed scale, a method
91 for accommodating the commonly encountered heteroscedasticity (Cunia, 1964) should be used. In a
92 recent analysis, using both weighted nonlinear regression and logarithmic transformation, Dutcă et al.

93 (2019) showed that the differences between parameter estimates for the two methods were minor
94 when appropriate weighting for heteroscedasticity was used. However, they concluded that the
95 weighted nonlinear approach is generally more versatile, being able to more easily address different
96 patterns of heteroscedasticity compared to logarithmic transformations which are limited in that sense.

97 Although ordinary least squares is assumed to be an unbiased estimator for regression model
98 parameters in the presence of heteroscedasticity, it may be a biased and inconsistent estimator of the
99 parameter variance-covariance matrix (Hayes and Cai, 2007; Parresol, 1993; White, 1980). However,
100 Mascaro et al. (2011) showed that the ignoring the heteroscedasticity in allometric biomass models
101 may cause systematic errors in predictions for small trees, because the small variance of small trees
102 means low leverage, if unweighted for heteroscedasticity. It was also shown that ignoring the
103 heteroscedasticity may result in erroneous confidence intervals of estimates (Saint-André et al., 2005),
104 which may further affect the uncertainty of biomass estimates. Nevertheless, it is not well known how
105 ignoring residual heteroscedasticity associated with allometric model may impact the estimates of
106 biomass over large forest areas.

107 For models with heteroscedastic residual variance such as the allometric biomass models
108 described in Eq. (1), the variance of ε_i is not constant (i.e., $var(\varepsilon_i) \neq \sigma^2$). Therefore, with weighted
109 least squares $var(\varepsilon_i|X_i) = \sigma^2 w_i$, where $w_i \propto \sigma_i^{-2}$ is a function that describes the weight for the i^{th}
110 observation. The weighting function should produce an estimate of the inverse of the variance for the
111 i^{th} observation ($w_i = \hat{\sigma}_i^{-2}$) and should always be positive. Therefore, weighted nonlinear least squares
112 regression allows residuals to have different variances but requires a function to describe the
113 heteroscedastic residual variance.

114 Multiple weighting functions have been proposed in the literature for allometric models. For
115 example, Cunia (1964) proposed a generic weighting function where the inverse of the predictor
116 variable to the power of 4, $w_i = D_i^{-4}$ or $w_i = (D_i^2 H_i)^{-2} = D_i^{-4} H_i^{-2}$ was used to compensate for
117 heteroscedasticity associated with tree volume model residuals. Other authors suggested $w_i = D_i^{-1}$ or
118 $w_i = D_i^{-2}$ as weighting functions for use with AGB or belowground allometric biomass models
119 (Kralicek et al., 2017). However, these functions with fixed parameters were shown to be

120 insufficiently flexible to describe the heteroscedasticity for any specific situation (Meng and Tsai,
121 1986; Williams and Gregoire, 1993). As a result, Meng and Tsai (1986) proposed a method to
122 specifically adjust the weights for each dataset, $w_i = (D_i^\lambda)^{-2}$ or $w_i = (D_i^\lambda H_i)^{-2}$, where λ is
123 estimated using maximum likelihood techniques. Williams and Gregoire (1993) recommended a more
124 general function $w_i = (D_i^{\lambda_2} H_i^{\lambda_3})^{-\lambda_1}$ which suggests that a function of predicted biomass,
125 $w_i = (\widehat{AGB}_i)^{-\lambda_1}$, can work as well, because the predicted AGB is itself a function of predictor
126 variables D and H. A version of a weighting function based on D, $w_i = (D_i)^{-k}$, is widely used
127 (Balboa-Murias et al., 2006; Huff et al., 2018; Huy et al., 2019; Vonderach et al., 2018) where the
128 parameter k can be estimated in many different ways. One way is to estimate the slope of a linear
129 model on the ln-ln scale, predicting $\ln(\varepsilon_i)$ where ε are the residuals from an unweighted model, as a
130 function of $\ln(D_i)$, where k is the estimated slope (Harvey, 1976; Park, 1966). Another way is to
131 divide the D_i observations into several classes (or groups, D_g) and then estimate the variance of AGB
132 observations within each class (σ_g^2); the parameter k is the slope of a linear model that predicts $\ln(\sigma_g^2)$
133 as a function of $\ln(D_g)$ (Picard et al., 2012). Dutcă et al. (2019) used a similar approach but based on
134 predicted AGB instead of D and on variances of residuals within groups from an unweighted model
135 instead of variance of AGB.

136 In the light of this wide range of choices, selecting a weighting approach can become a rather
137 difficult decision. In this paper we review multiple weighting approaches for nonlinear allometric
138 biomass models and assess their effectiveness for accommodating heteroscedasticity for multiple
139 biomass datasets. Furthermore, using a calibration dataset consisting of measurements of AGB, D and
140 H, coupled with an inventory dataset consisting of measurements of D and H for all trees on plots, we
141 assess the sensitivity of large area biomass estimates to the effects of the following analytical factors:
142 (i) ignoring or dealing with heteroscedasticity, (ii) ignoring or accommodating allometric model
143 prediction uncertainty, and (iii) use of D versus D and H as model predictor variables.

144

145 **2. Material and methods**

146 **2.1. Data**

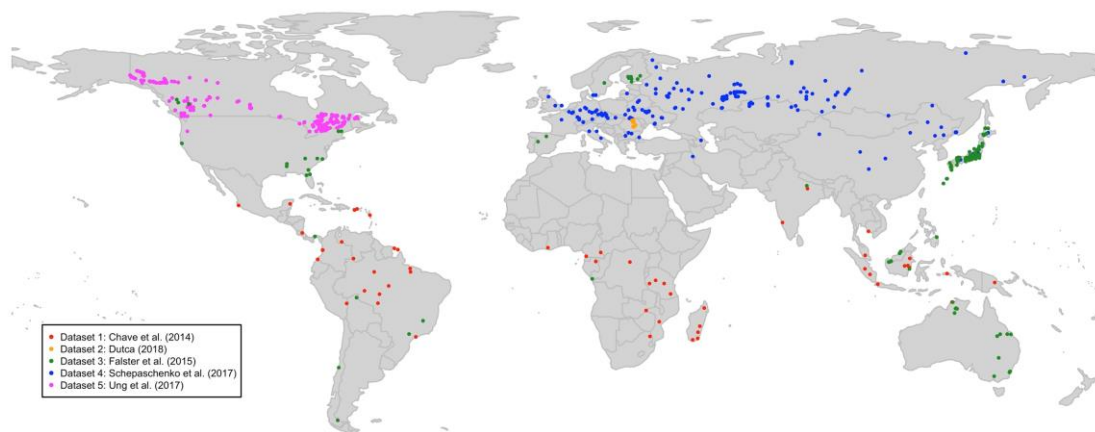
147 For testing the effectiveness of the weighting approaches, we used six biomass datasets, whereas for
148 assessing the sensitivity of large area biomass estimates to the effects of the weighting approaches we
149 used a biomass calibration dataset to calibrate the models and an inventory dataset to assess the
150 effects on large area estimates.

151

152 **2.1.1. Biomass datasets for testing the efficiency of weighting approaches**

153 The five biomass datasets used in this study are from different regions of the world (Fig. 1). Dataset 6
154 consists of the merger of Datasets 1, 3, 4 and 5. Dataset 2 was not included in the merged dataset
155 because it used a different definition for D. For each dataset we fit allometric biomass models that
156 incorporated weighting to accommodate heteroscedasticity, and then tested the effectiveness of the
157 weighting approaches for accommodating heteroscedasticity. Information such as the sample size and
158 the range of D, H, AGB and latitude for the datasets are presented in Table 1.

159



160

161 **Fig. 1.** The distribution of sampling sites by dataset

162

163 **Table 1**

164 The biomass datasets.

Dataset	Species	Latitude range (Deg.)	Sample size	D range (cm)	H range (m)	AGB range (kg)	References
---------	---------	-----------------------	-------------	--------------	-------------	----------------	------------

Dataset 1	Multiple	-24.9, 25.0	4004	5.0–212.0	1.2–70.7	1.2–76063.5	(Chave et al., 2014)
Dataset 2	Norway spruce	45.4, 47.6	240	0.6–10.0*	0.5–5.5	0.1–15.5	(Dutcă, 2018)
Dataset 3	Multiple	-51.6, 62.3	3489	5.0–139.6	1.5–46.5	0.4–16418.4	(Falster et al., 2015)
Dataset 4	Multiple	31.5, 69.9	5144	5.0–72.9	2.3–42.8	0.6–4291.3	(Schepaschenko et al., 2017)
Dataset 5	Multiple	43.9, 64.0	8659	5.0–74.3	2.5–52.2	2.2–2951.4	(Ung et al., 2017)
Dataset 6	Multiple	-51.6, 64.0	21296	5.0–212.0	1.2–70.7	0.4–76 063.5	Datasets 1, 2, 4 and 5

165 *Dataset 2 (Dutcă, 2018) uses diameter at collar height instead of diameter at breast height.

166

167 **2.1.2. Data for assessing the sensitivity of large area biomass estimates to the effects of the**
168 **weighting approaches**

169 To investigate the sensitivity of large area biomass estimates to the effects of methods for
170 accommodating heteroscedasticity, we used a calibration sample to fit the weighted allometric model
171 and then used the resulting model to predict individual tree biomass for trees in the inventory sample.

172

173 **i) The calibration sample**

174 The calibration sample is a subset of Dataset 4 (Table 1, Schepaschenko et al. 2017), containing data
175 for only Norway spruce trees. The calibration dataset includes measurements of D ranging from 5.0 to
176 67.6 cm, measurements of H ranging from 4.0 to 42.8 m and measurements of AGB ranging from 4.9
177 to 3364.2 kg for 503 Norway spruce trees from several European countries.

178

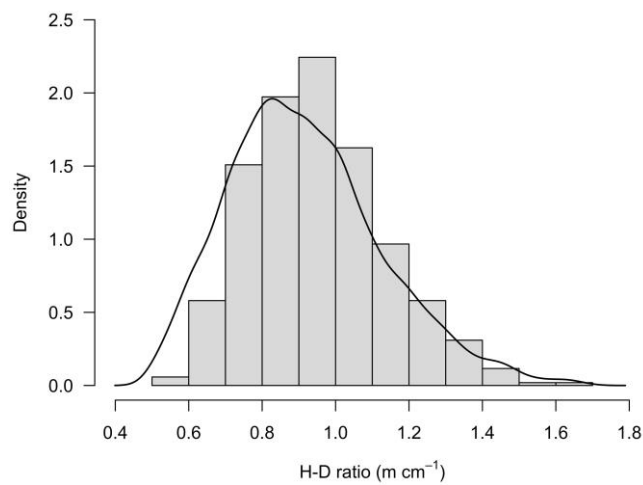
179 **ii) The inventory sample**

180 The inventory sample consists of measurements of D and H for trees on 243 sample plots from
181 Romania. The inventory dataset was used with the calibration dataset to assess the effects of
182 weighting approaches on large area biomass estimates. The 243 sample plots were selected from the
183 Romanian National Forest Inventory (NFI) and included only Norway spruce trees. Norway spruce is
184 an important species for Romania, often found in pure stands but also in mixtures, covering
185 approximately 1.3 million ha (19% of Romanian forests). Because the Romanian NFI uses a 4 km by
186 4 km grid-based sampling design in the mountain area where pure Norway spruce grows (Marin et al.,
187 2020), the 243 plots represent 388.8 thousand hectares of forest. The circular sample plots are located
188 at the intersections of the grid lines and have a radius of 12.62 m with an area of 500 m². For each

189 plot, D and H were measured for all trees with $D > 28.5$ cm. For a smaller, concentric circular subplot
 190 of radius 7.98 m and area of 200 m^2 , D and H were also measured for trees with $5.6 \leq D \leq 28.5$ cm.

191 Relationships for datasets with different H-D ratios (H, in m, divided by D, in cm) may
 192 require different model forms. Therefore, to ensure a model developed for the calibration dataset is
 193 applicable to the inventory data, H-D ratios for the two datasets were compared. Figure 2 shows good
 194 agreement between the histogram (i.e., the calibration sample) and the density curve (i.e., the
 195 inventory sample).

196



197

198 **Fig. 2.** The distribution of H-D ratio for the calibration sample (histogram) and the inventory sample (density line)

199

200 The H-D ratio (in m cm^{-1}) ranged between 0.36 and 2.56 for the calibration sample and
 201 between 0.42 and 2.11 for the inventory sample. The ranges of D and H for the inventory and
 202 calibration samples were also similar (Table 1 and section 2.1.2), varying between 5.6 to 72.2 cm for
 203 D and between 3.1 and 47.5 m for H.

204

205 **2.2. Statistical analysis**

206 **2.2.1. Modelling AGB and heteroscedasticity**

207 We modelled AGB using two allometric biomass model forms:

208 (a) Using D as the single predictor variable (Asrat et al., 2020):

209
$$AGB = \beta_{01} \cdot D^{\beta_{11}} + \varepsilon_1 \quad (2)$$

210 (b) Using both D and H as predictor variables (Dutcă et al., 2019):

211
$$AGB = \beta_{02} \cdot D^{\beta_{12}} \cdot H^{\beta_{22}} + \varepsilon_2 \quad (3)$$

212 where AGB, D, and H are as previously defined; the β s are the model parameters to be estimated; and

213 ε_1 and ε_2 are random residual terms. Initially, we fit these models without accommodation for

214 heteroscedasticity. However, because the residuals for Eq. (2) and Eq. (3) usually exhibit

215 heteroscedasticity, multiple weighting procedures were considered (Table 2).

216

217 **Table 2**

218 The weighting procedures tested.

Weighting procedure	Weighting variable	Computation details
For Eqs. (2) and (3)		
1	$w_i = \frac{1}{D_i}$	The weight of the i^{th} observation (w_i) was calculated as the inverse of diameter (D_i) (Kralicek et al., 2017).
2	$w_i = \frac{1}{D_i^2}$	The inverse of D_i^2 (Kralicek et al., 2017; Meng and Tsai, 1986).
3	$w_i = \frac{1}{D_i^4}$	The inverse of D_i^4 (Cunia, 1964).
4	$w_i = \frac{1}{D_i^\lambda}$	Prediction of heteroscedastic variance as a function of D. This approach was proposed by (Harvey, 1976; Park, 1966), and consists of multiple steps: (i) fit a nonlinear unweighted model and calculate the squared residual for the i^{th} tree ($\hat{\varepsilon}_i^2$); (ii) ln-ln transform the $\hat{\varepsilon}_i^2$ and D_i values; (iii) fit a linear model: $\ln(\hat{\varepsilon}_i^2) = \alpha + \lambda \cdot \ln(D_i) + \varepsilon$; (iv) using the slope λ and D_i to calculate the weight of i^{th} tree.
5	$w_i = \frac{1}{D_i^\lambda}$	Prediction of heteroscedastic variance as a function of D, using a grouping approach (Picard et al., 2012): (i) divide the D observations into u classes ($u = 5$), centred on D_u ; (ii) calculate the variance of AGB for each class (σ_u^2); (iii) ln-ln transform the σ_u^2 and D_u values; (iv) fit a linear model: $\ln(\sigma_u^2) = \alpha + \lambda \cdot \ln(D_u) + \varepsilon$; (v) use the slope λ and D_i to calculate the weight of i^{th} tree.
6	$w_i = \frac{1}{D_i^\lambda}$	Prediction of heteroscedastic variance as a function of D, using a grouping method (McRoberts and Westfall, 2014): (i) fitting an unweighted nonlinear model to data and calculate the heteroscedastic residuals ($\hat{\varepsilon}_i$); (ii) sort the pairs D_i and $\hat{\varepsilon}_i$ in ascending order with respect to D_i ; (iii) group the pairs D_i and $\hat{\varepsilon}_i$ in u groups of size 25; (iv) for each group, calculate the mean of D_i (\overline{D}_u) and the variance of $\hat{\varepsilon}_i$ (σ_u^2); (v) ln-ln transform the σ_u^2 and \overline{D}_u values; (vi) fit a linear model: $\ln(\sigma_u^2) = \alpha + \lambda \cdot \ln(\overline{D}_u) + \varepsilon$; (vii) use the parameter λ and D_i to compute the weight of i^{th} tree.
7	$w_i = \frac{1}{D_i^\lambda}$	Prediction of heteroscedastic variance as a function of D, in two stages, and using a grouping method: (i) fit a weighted nonlinear model (using the weights from procedure #6) and calculate the heteroscedastic residuals ($\hat{\varepsilon}_i$); (ii) sort the pairs D_i and $\hat{\varepsilon}_i$ in ascending order with respect to D_i ;

		<ul style="list-style-type: none"> (iii) group the pairs D_i and $\hat{\epsilon}_i$ in u groups of size 25; (iv) for each group, calculate the mean of D_i (\overline{D}_u) and the variance of $\hat{\epsilon}_i$ (σ_u^2); (v) ln-ln transform the σ_u^2 and \overline{D}_u values; (vi) fit a linear model: $\ln(\sigma_u^2) = \alpha + \lambda \cdot \ln(\overline{D}_u) + \epsilon$; (vii) use the parameter λ and D_i to compute the weight of i^{th} tree.
8	$w_i = \frac{1}{\overline{AGB}_i^\lambda}$	<p>Prediction of heteroscedastic variance as a function of predicted AGB (Dutcă et al., 2019; McRoberts and Westfall, 2014). This is similar to procedure #6, however, predicted AGB is used instead of D as predictor of variance:</p> <ul style="list-style-type: none"> (i) fitting an unweighted nonlinear model to data and calculate the predicted AGB (\overline{AGB}_i) and the heteroscedastic residuals ($\hat{\epsilon}_i$); (ii) sort the pairs \overline{AGB}_i and $\hat{\epsilon}_i$ in ascending order with respect to \overline{AGB}_i; (iii) group the pairs \overline{AGB}_i and $\hat{\epsilon}_i$ in u groups of size 25; (iv) for each group, calculate the mean of \overline{AGB}_i (\overline{AGB}_u) and the variance of $\hat{\epsilon}_i$ (σ_u^2); (v) ln-ln transform the σ_u^2 and \overline{AGB}_u values; (vi) fit a linear model: $\ln(\sigma_u^2) = \alpha + \lambda \cdot \ln(\overline{AGB}_u) + \epsilon$; (vii) use the parameter λ and \overline{AGB}_i (from first step) to compute the weight of i^{th} tree.
9	$w_i = \frac{1}{\overline{AGB}_i^\lambda}$	<p>Prediction of heteroscedastic variance as a function of predicted AGB, in two stages, and using a grouping method:</p> <ul style="list-style-type: none"> (i) fitting a weighted nonlinear model (using the weights from procedure #8) and calculate the predicted AGB (\overline{AGB}_i) and the heteroscedastic residuals ($\hat{\epsilon}_i$); (ii) sort the pairs \overline{AGB}_i and $\hat{\epsilon}_i$ in ascending order with respect to \overline{AGB}_i; (iii) group the pairs \overline{AGB}_i and $\hat{\epsilon}_i$ in u groups of size 25; (iv) for each group, calculate the mean of \overline{AGB}_i (\overline{AGB}_u) and the variance of $\hat{\epsilon}_i$ (σ_u^2); (v) ln-ln transform the σ_u^2 and \overline{AGB}_u values; (vi) fit a linear model: $\ln(\sigma_u^2) = \alpha + \lambda \cdot \ln(\overline{AGB}_u) + \epsilon$; (vii) use the parameter λ and \overline{AGB}_i (from first step) to compute the weight of i^{th} tree.
10	$w_i = \frac{1}{[\exp(\ln(\overline{AGB})_i)]^2}$	<p>Using the predicted AGB (from a ln-ln transformed model) as a predictor of heteroscedastic variance:</p> <ul style="list-style-type: none"> (i) fit a linear model on ln-ln transformed data (Eq. 4 or Eq. 5); (ii) calculate the predicted ln(AGB) of i^{th} tree (i.e. $\ln(\overline{AGB})_i$); (iii) calculate the weight of i^{th} tree as the inverse of squared back-transformed AGB. Including the back transformation correction factor (Baskerville, 1972; Goldberger, 1968; Sprugel, 1983) is not necessary since the correction factor is a constant and, therefore, would have a redundant effect.
<hr/>		
Only for Eq. (3)		
11	$w_i = \frac{1}{D_i^4 H_i^2}$	The inverse of squared D^2H (Cunia, 1964; Jacobs and Monteith, 1981).
12	$w_i = \frac{1}{(D_i^2 H_i)^\lambda}$	<p>Prediction of heteroscedastic variance as a function of D^2H, using a grouping method:</p> <ul style="list-style-type: none"> (i) fitting an unweighted nonlinear model, $AGB = f(D^2H)$, to data and calculate the heteroscedastic residuals ($\hat{\epsilon}_i$); (ii) sort the pairs D^2H_i and $\hat{\epsilon}_i$ in ascending order with respect to D^2H_i; (iii) group the pairs D^2H_i and $\hat{\epsilon}_i$ in u groups of size 25; (iv) for each group, calculate the mean of D^2H_i ($\overline{D^2H}_u$) and the variance of $\hat{\epsilon}_i$ (σ_u^2); (v) fit a nonlinear model: $\ln(\sigma_u^2) = \alpha + \lambda \cdot \overline{D^2H}_u + \epsilon$; (vi) use the parameter estimate λ to compute the weight of i^{th} tree.
13	$w_i = \frac{1}{D_i^{\lambda_1} H_i^{\lambda_2}}$	<p>Prediction of heteroscedastic variance as a function of D and H, adapted after (Harvey, 1976; Park, 1966):</p> <ul style="list-style-type: none"> (i) fitting an unweighted nonlinear model as in Eq. (3), and calculate the heteroscedastic residuals ($\hat{\epsilon}_i$); (ii) ln-ln transform $\hat{\epsilon}_i$, D and H;

- (iii) fit a linear model: $\ln(\hat{\epsilon}_i^2) = \alpha + \lambda_1 \cdot \ln(D) + \lambda_2 \cdot \ln(H) + \epsilon$;
- (iv) use the slopes estimates λ_1 and λ_2 to compute the weight of i^{th} tree.

14

$$w_i = \frac{1}{D_i^{\lambda_1} H_i^{\lambda_2}}$$

Prediction of heteroscedastic variance as a function of D and H, using a grouping approach:

- (i) fit a linear model to predict $\ln(AGB)$ as a function of $\ln(D)$ and $\ln(H)$;
- (ii) calculate the back transformed predicted AGB using a correction factor: $\overline{AGB} = \exp(\ln(\overline{AGB})) \cdot \exp(0.5 \cdot RSE^2)$, where RSE is the residual standard error of the model in ln-ln scale;
- (iii) calculate the heteroscedastic residuals ($\hat{\epsilon}_i$) as difference between observed AGB and predicted AGB;
- (iv) sort the triple D_i , H_i and $\hat{\epsilon}_i$ in ascending order with respect to D_i ;
- (v) group the triple D_i , H_i and $\hat{\epsilon}_i$ in u groups of size 25;
- (vi) for each group, calculate the mean of D_i (\overline{D}_u), mean of H_i (\overline{H}_u) and the variance of $\hat{\epsilon}_i$ (σ_u^2);
- (vii) ln-ln transform the \overline{D}_u , \overline{H}_u and σ_u^2 values;
- (viii) fit a linear model: $\ln(\sigma_u^2) = \alpha + \lambda_1 \cdot \ln(\overline{D}_u) + \lambda_2 \cdot \ln(\overline{H}_u) + \epsilon$;
- (ix) use the slopes λ_1 and λ_2 to compute the weight of i^{th} tree.

219

220 In addition to these nonlinear weighting procedures, we also tested the ln-ln transformation as a way
 221 to accommodate heteroscedasticity. The ln-ln transformed models corresponding to Eq. (2) and (3)
 222 were:

$$223 \quad \ln(AGB) = b_{01} + b_{11} \cdot \ln(D) + \epsilon_1 \quad (4)$$

$$224 \quad \ln(AGB) = b_{02} + b_{12} \cdot \ln(D) + b_{22} \cdot \ln(H) + \epsilon_2 \quad (5)$$

225 where ϵ_1 and ϵ_2 are random, normally distributed residuals but not the same residuals as for Eq. (2)
 226 and Eq. (3). When back-transforming Eqs. (4) and (5), the distribution of residuals becomes
 227 lognormal. Further, back-transforming induces systematic error into predictions on the original scale
 228 with the result that a correction factor is required. We adopted the correction factor $CF = \exp(0.5 \cdot$
 229 $RSE^2)$, where RSE is the residual standard error on the ln-ln scale (Baskerville, 1972; Goldberger,
 230 1968).

231

232 2.2.3. Testing the effectiveness of weighting procedures

233 The Breusch-Pagan test is widely used to test for heteroscedasticity in linear models (Breusch and
 234 Pagan, 1979). We adapted the Breusch-Pagan test for nonlinear weighted models using the following
 235 steps:

- 236 (i) calculate the weighted residuals, (\widehat{ew}_i), resulting from the nonlinear model predictions:

$$237 \quad \widehat{ew}_i = (AGB_i - \overline{AGB}_i) \cdot \sqrt{w_i} \quad (6)$$

238 where AGB_i is the observed AGB for the i^{th} tree; \widehat{AGB}_i is the predicted AGB for the i^{th} tree; w_i
239 is the same weight for the i^{th} tree as was used to fit the nonlinear model. For the unweighted
240 model, $\sqrt{w_i} = 1$.

241 (ii) define the auxiliary linear models that predict squared weighted residuals as a function of the
242 predictor variable(s):

$$243 \quad \widehat{ew}_i^2 = a_1 + b_1D + \varepsilon \quad (7)$$

$$244 \quad \widehat{ew}_i^2 = a_2 + b_2D + c_2H + \varepsilon \quad (8)$$

245 (iii) retain the R^2 values for these linear models and use them to calculate χ^2 :

$$246 \quad \chi^2 = n_b \cdot R^2 \quad (9)$$

247 where, n_b is the sample size of biomass datasets.

248 (iv) calculate the p-value of the χ^2 statistic, using the right tail of a χ^2 distribution with $df = 1$ for
249 Eq. 7 and $df = 2$ for Eq. 8, degrees of freedom. The null hypothesis of homoscedasticity is
250 rejected if $p < 0.05$.

251

252 **2.3. Assessing the sensitivity of large area biomass estimates to the effects of the weighting** 253 **procedures**

254 To assess the sensitivity of large area biomass estimates to the effects of the weighting procedures we
255 used a probability sample (i.e., the inventory sample) together with a calibration sample (see section
256 2.1.2). However, because the simple expansion estimator (Cochran, 1977, p.157; Särndal et al., 1992,
257 p.104) is unbiased under the assumption of at most negligible uncertainty in the plot-level AGB
258 values, and because this assumption may or may not be appropriate, depending on the level of
259 uncertainty in the allometric model parameter estimates and residuals, we considered two options
260 when estimating the uncertainty of large area biomass estimates: (i) model prediction uncertainty is
261 ignored (excluded) and (ii) model prediction uncertainty is included.

262

263 **2.3.1. Ignoring model prediction uncertainty**

264 When the model prediction uncertainty was not included, the AGB of every tree in every plot was
 265 predicted based on the parameter estimates of Eq. (2) and Eq. (3), that either included or excluded
 266 weighting for heteroscedasticity (Table 2). For the ln-ln transformation approach we used the back
 267 transformed prediction from Eq. (4) and Eq. (5). Assuming an equal probability sample, the
 268 population mean AGB per hectare ($\hat{\mu}$) and the standard error of the mean ($SE(\hat{\mu})$) were estimated
 269 using a simple expansion estimator:

$$270 \quad \hat{\mu} = \frac{1}{n} \sum_{j=1}^n \widehat{AGB}_j \quad (10)$$

$$271 \quad SE(\hat{\mu}) = \sqrt{\frac{1}{n(n-1)} \sum_{j=1}^n (\widehat{AGB}_j - \hat{\mu})^2} \quad (11)$$

272 where \widehat{AGB}_j is the predicted AGB of the j^{th} plot (j is the plot index); n is the total number of plots.

273

274 **2.3.2. Assessing the effects of allometric model prediction uncertainty**

275 The simple expansion estimators (Eq. 10 and Eq. 11) were used under the assumption of, at most,
 276 negligible uncertainty in the plot-level AGB values. However, because the plot-level AGB values
 277 were obtained by summation of within plot individual tree predictions, this assumption may not be
 278 reasonable. Therefore, we used a form of “hybrid inference” (Condés and McRoberts, 2017;
 279 McRoberts et al., 2019, 2016, 2015; Ståhl et al., 2016) to incorporate both model prediction
 280 uncertainty and sampling variability. Because the inventory sample consisted of sample plots for
 281 which individual tree biomass was not measured, we used the calibration sample to predict the
 282 biomass of the trees inside the plots to obtain plot biomass predictions. However, because the plot
 283 biomass was not measured but predicted, we used a Monte-Carlo procedure to propagate uncertainty
 284 from model parameter estimates and residuals to large area biomass estimates and their standard
 285 errors. Because the variance-covariance matrix for the model parameter estimates is usually based on
 286 linear approximations using Taylor series, which may be biased for nonlinear models (McRoberts and
 287 Westfall, 2014), we used a bootstrap approach within the Monte Carlo procedure instead of the more
 288 commonly used estimated variance-covariance matrix. The following steps describe the Monte-Carlo
 289 error propagation procedure:

290 Step (1) Select a simple random bootstrap resample (using “bootstrap residuals” approach) of trees
 291 with replacement from the calibration sample and fit the model using weighted least
 292 squares. For the “bootstrap residuals” procedure, we calculated the weighted residuals as in
 293 Eq. (6). The vector of weighted residuals was resampled with replacement, to obtain the
 294 resampled weighted residuals. The resampled residuals were added to the predicted AGB
 295 (obtained from the weighted nonlinear model fitted to the original calibration dataset), to
 296 obtain the resampled AGB. The vector of resampled AGB was further merged with the
 297 vectors of the two predictor variables, D and H, to form the resampled AGB dataset. A
 298 weighted nonlinear model was further fitted to the resampled AGB dataset. For ln-ln
 299 transformation (Eqs. 4 and 5), since the transformation is assumed to produce
 300 homoscedastic residuals, we resampled the ln-ln transformed dataset and fitted an allometric
 301 model (in ln-ln scale) to the resampled dataset.

302 Step (2) Select a simple random bootstrap resample of plots with replacement from the inventory
 303 sample;

304 Step (3) For every tree on every plot in the inventory sample from step (2):
 305 (3.a) predict the individual tree biomass using the parameters estimated from step (1);
 306 (3.b) add a random heteroscedastic residual. A value was randomly selected from a normal
 307 distribution $N(0, 1)$, which was truncated to the interval $[-3, 3]$. The selected random value
 308 was further multiplied by the predicted heteroscedastic residual standard deviation. To
 309 model the standard deviation of heteroscedastic residuals we used a similar approach to
 310 modelling heteroscedasticity (see Table 2).

311 Step (4) Add the tree-level predictions to obtain plot-level biomass predictions for all plots selected
 312 in step (2) and scale the plot-level biomass prediction to a per unit area basis.

313 Step (5) For the rep^{th} repetition, estimate mean AGB per hectare ($\hat{\mu}^{rep}$) and the variance of the mean
 314 ($\widehat{\text{var}}(\hat{\mu}^{rep})$) from the plot-level scaled biomass predictions from step (5):

$$315 \quad \hat{\mu}^{rep} = \frac{1}{n} \sum_{j=1}^n \widehat{AGB}_j^{rep} \quad (12)$$

316 where rep is the repetition index, n is the total number of plots (i.e., n = 243), \widehat{AGB}_j^{rep} is the
 317 predicted AGB of the jth plot scaled to hectare, for repth repetition. The variance of the mean
 318 AGB per hectare (i.e., the within simulation variance) was estimated as:

$$319 \quad \widehat{var}(\hat{\mu}^{rep}) = \frac{1}{n(n-1)} \sum_{j=1}^n (\widehat{AGB}_j^{rep} - \hat{\mu}^{rep})^2 \quad (13)$$

320 Step (6) Repeat steps (1)-(5) many times ($n_{rep} = 5000$). The population mean AGB per hectare ($\hat{\mu}$),
 321 the mean of within simulation variance ($\overline{\widehat{var}(\hat{\mu}^{rep})}$), the between simulation variance
 322 ($\widehat{var}(\hat{\mu})$) were calculated as:

$$323 \quad \hat{\mu} = \frac{1}{n_{rep}} \sum_{rep=1}^{n_{rep}} \hat{\mu}^{rep} \quad (14)$$

$$324 \quad \overline{\widehat{var}(\hat{\mu}^{rep})} = \frac{1}{n_{rep}} \sum_{rep=1}^{n_{rep}} \widehat{var}(\hat{\mu}^{rep}) \quad (15)$$

$$325 \quad \widehat{var}(\hat{\mu}) = \left(1 + \frac{1}{n_{rep}}\right) \cdot \frac{1}{n_{rep}-1} \sum_{rep=1}^{n_{rep}} (\hat{\mu}^{rep} - \hat{\mu})^2 \quad (16)$$

326 Step (7) Replicate steps (1)-(6) until the estimate of mean AGB per hectare (Eq. 14) and the
 327 variances presented in Eq. (15) and Eq. (16) stabilize. For each additional replication we
 328 calculated the mean of $\hat{\mu}$, mean of $\overline{\widehat{var}(\hat{\mu}^{rep})}$ and mean of $\widehat{var}(\hat{\mu})$ over the executed
 329 replications. The replications continued until the largest difference between any two values
 330 of means of $\hat{\mu}$, means of $\overline{\widehat{var}(\hat{\mu}^{rep})}$ and respectively means of $\widehat{var}(\hat{\mu})$, for the last 30% of
 331 replications, were less than 5%, however, executing not less than 500 replications. We
 332 further reported the mean of $\hat{\mu}$ over the stabilization replications (i.e., the stabilized mean)
 333 and the standard error of the mean, calculated based on stabilized variances (Eq. 15 and Eq.
 334 16):

$$335 \quad SE(\hat{\mu}) = \sqrt{\overline{\widehat{var}(\hat{\mu}^{rep})} + \widehat{var}(\hat{\mu})} \quad (17)$$

336 Statistical analysis was performed in R (R Core Team, 2017) with the RStudio interface (RStudio
 337 Team, 2016) and using the package ‘MASS’ (Venables et al., 2002).

338 **3. Results**

339 **3.1. Testing weighting procedures**

340 The results of the Breusch-Pagan test for heteroscedasticity are presented in Table 3. When $p < 0.05$
 341 the null hypothesis of homoscedasticity was rejected, and the residuals were assumed to exhibit
 342 heteroscedasticity, whereas when $p > 0.05$ we assumed homoscedastic residuals. The models that
 343 ignored heteroscedasticity (weighting procedure 0, Table 3) produced statistically significant
 344 Breusch-Pagan test results for all datasets (and model forms), thereby justifying accommodation for
 345 heteroscedasticity.

346

347 **Table 3**

348 The Breusch-Pagan test results (p-values of the test), by dataset, model form and weighting procedure.

Model form	Weighting procedure	Weighting variable	Dataset 1	Dataset 2	Dataset 3	Dataset 4	Dataset 5	Dataset 6
<i>AGB</i> $= \beta_0 \cdot D^{\beta_1} + \varepsilon$	0 ^a	N.A.	<0.001	<0.001	<0.001	<0.001	<0.001	<0.001
	1	D^{-1}	<0.001	<0.001	<0.001	<0.001	<0.001	<0.001
	2	D^{-2}	<0.001	<0.001	<0.001	<0.001	<0.001	<0.001
	3	D^{-4}	<0.001	<0.001	<0.001	<0.001	<0.001	<0.001
	4	$D^{-\lambda}$	<0.001	<0.001	<0.001	0.192	<0.001	<0.001
	5	$D^{-\lambda}$	<0.001	<0.001	<0.001	<0.001	<0.001	<0.001
	6	$D^{-\lambda}$	0.151	0.293	<0.001	0.023	0.602	0.282
	7	$D^{-\lambda}$	0.093	0.412	0.202	0.623	0.519	0.288
	8	$\overline{AGB}^{-\lambda}$	0.265	0.434	0.720	0.477	0.951	<0.001
	9	$\overline{AGB}^{-\lambda}$	0.202	0.649	0.321	0.389	0.970	0.584
	10	$[\exp(\ln(\overline{AGB}))]^{-2}$	0.014	0.492	0.011	0.029	0.007	<0.001
15 ^b	N.A.	<0.001	0.726	<0.001	<0.001	<0.001	0.681	
<i>AGB</i> $= \beta_0 \cdot D^{\beta_1} \cdot H^{\beta_2} + \varepsilon$	0 ^a	N.A.	<0.001	<0.001	<0.001	<0.001	<0.001	<0.001
	1	D^{-1}	<0.001	<0.001	<0.001	<0.001	<0.001	<0.001
	2	D^{-2}	<0.001	<0.001	<0.001	<0.001	<0.001	<0.001
	3	D^{-4}	<0.001	<0.001	<0.001	<0.001	<0.001	<0.001
	4	$D^{-\lambda}$	<0.001	0.006	<0.001	<0.001	<0.001	<0.001
	5	$D^{-\lambda}$	<0.001	<0.001	<0.001	<0.001	<0.001	<0.001
	6	$D^{-\lambda}$	<0.001	0.010	0.021	0.003	<0.001	<0.001
	7	$D^{-\lambda}$	<0.001	0.126	0.026	0.104	<0.001	<0.001
	8	$\overline{AGB}^{-\lambda}$	<0.001	<0.001	0.034	0.001	<0.001	<0.001
	9	$\overline{AGB}^{-\lambda}$	0.156	0.013	0.001	<0.001	<0.001	<0.001
	10	$[\exp(\ln(\overline{AGB}))]^{-2}$	<0.001	0.010	<0.001	<0.001	<0.001	<0.001
	11	$D^{-4}H^{-2}$	<0.001	<0.001	<0.001	<0.001	<0.001	<0.001
	12	$(D^2H)^{-\lambda}$	<0.001	<0.001	<0.001	<0.001	<0.001	<0.001
	13	$D^{-\lambda_1}H^{-\lambda_2}$	<0.001	0.002	<0.001	<0.001	<0.001	<0.001
	14	$D^{-\lambda_1}H^{-\lambda_2}$	0.376	0.084	0.158	0.141	<0.001	<0.001
15 ^b	N.A.	<0.001	0.047	<0.001	<0.001	<0.001	<0.001	

349 ^a No weighting; ^b Ln-ln transformation.

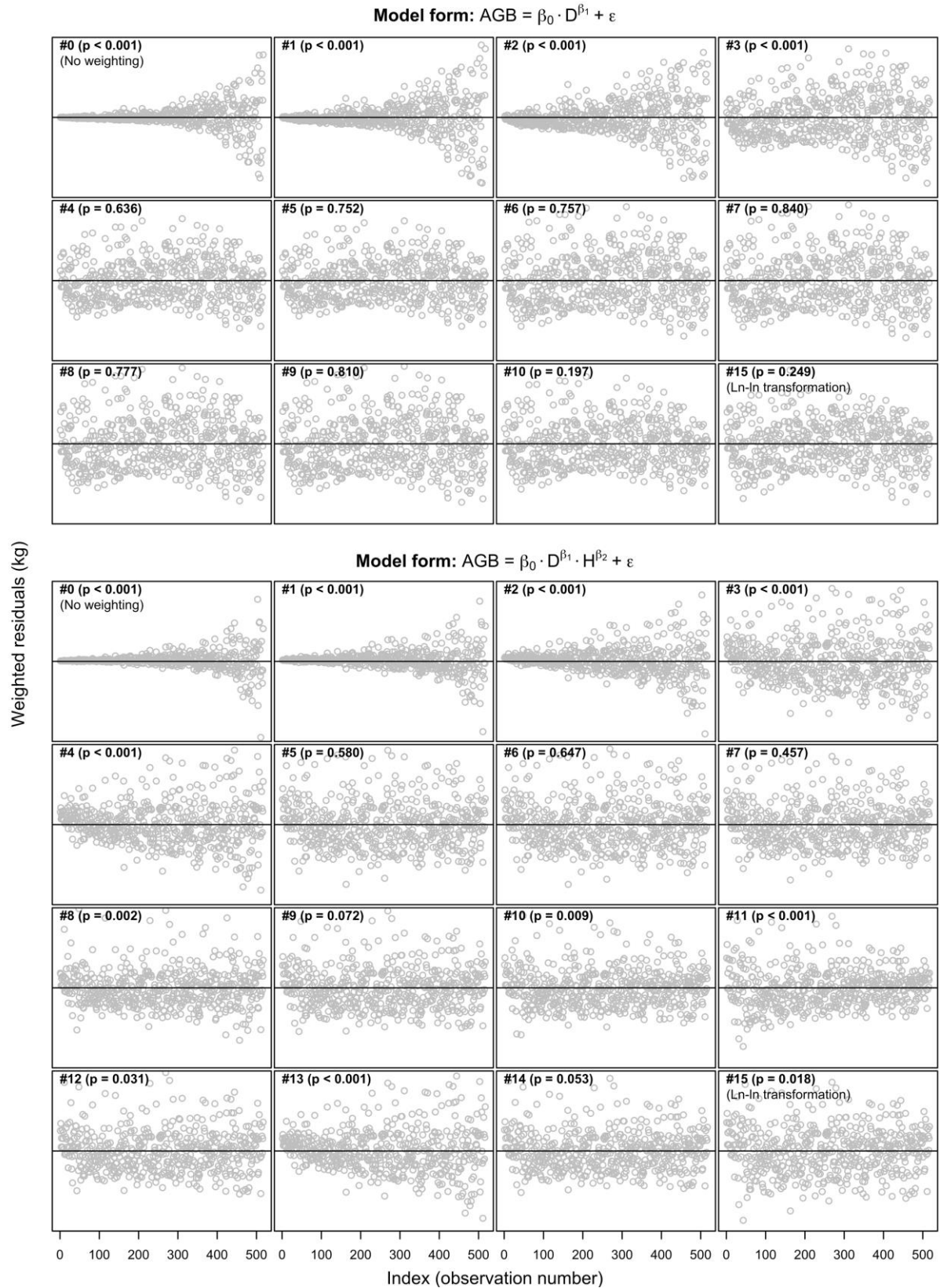
350

351 The large number of p-values greater than 0.05 for models based on single predictors (Eq. 2,
352 models based on D only) suggests that the tested weighting procedures are more effective for single
353 predictor models. For the single predictor models, the two weighting procedures that predicted the
354 variance in two stages (procedures 7 and 9), successfully accommodated heteroscedasticity for all
355 datasets. However, for models based on two predictors (Eq. 3), weighting procedure 7 accommodated
356 heteroscedasticity for only three of seven datasets (if including here the calibration dataset, Fig. 3),
357 procedure 9 was effective for only two of seven datasets, whereas procedure 14 that predicts
358 heteroscedastic variance as a function of both D and H was the most effective, accommodating
359 heteroscedasticity for five of seven datasets (Table 3 and Fig. 3).

360 Logarithmic transformation was not very effective in accommodating heteroscedasticity. For
361 models based on D (Eq. 2), the heteroscedasticity was satisfactorily accommodated for three of seven
362 datasets, whereas for Eq. (3) the ln-ln transformation resulted in statistically significant
363 heteroscedasticity for all datasets (Table 3 and Fig. 3).

364 For the calibration dataset, the results of the Breusch-Pagan test are presented in Fig. 3, along
365 with the weighted residuals. The residuals were relatively homoscedastic when the p-value was larger
366 than 0.05. It can also be observed that the unweighted residuals (weighting procedure 0, Fig. 3) were
367 heavily heteroscedastic ($p < 0.001$), with the variance increasing as tree size increased. Moreover, for
368 single predictor models slight systematic lack of fit can be observed but was mostly eliminated by
369 addition of H as a model predictor variable. Logarithmic transformation (i.e., procedure 15, Fig. 3)
370 produced relatively homoscedastic residuals for both model forms, although for models based on both
371 D and H (Eq. 3) the p-value was just below the significance level ($p = 0.018$) which suggests
372 heteroscedasticity.

373



374

375

Fig. 3. The weighted residuals (expressed in kg) by index of observation for the calibration sample, shown for each model

376

form and each weighting procedure (see Table 2). Note: The labels on y-axis not shown because the range differs by

377

graph.

378

379 **3.2. The effects of weighting procedures on large area biomass estimates**

380 The large-area biomass estimates were affected by the weighting approach to a moderate degree. For
 381 the models of Eq. (2) and Eq. (3), the weighting procedures and the sources of uncertainty considered,
 382 the estimates of mean AGB per hectare varied between 177.45 Mg ha⁻¹ and 188.47 Mg ha⁻¹ (Table 4),
 383 i.e., with a range of 11.02 Mg ha⁻¹ (i.e., 6.2%). However, this range is less than the 95% confidence
 384 interval width estimated using the smallest SE (Table 4) which suggests that these differences are due
 385 to random effects rather than any bias in the estimation procedure.

386

387 **Table 4**

388 Estimates of mean AGB per hectare ($\hat{\mu}$) and the standard error of the estimate of mean (SE($\hat{\mu}$)), in Mg ha⁻¹, by weighting
 389 procedure, excluding, and including model prediction uncertainty, for models based on Eq. (2) and Eq. (3).

Weighting procedure	Predictor variable: D (Eq. 2)				Predictor variables: D and H (Eq. 3)			
	Excluding model prediction uncertainty		Including model prediction uncertainty		Excluding model prediction uncertainty		Including model prediction uncertainty	
	$\hat{\mu}$	SE($\hat{\mu}$)	$\hat{\mu}$	SE($\hat{\mu}$)	$\hat{\mu}$	SE($\hat{\mu}$)	$\hat{\mu}$	SE($\hat{\mu}$)
0 ^a	182.13	7.75	183.32	11.23	179.35	8.39	181.50	12.05
1	183.66	7.76	183.70	11.09	181.17	8.36	183.01	11.93
2	183.85	7.76	183.33	11.05	182.36	8.28	183.62	11.79
3	185.38	7.92	185.21	14.99	181.96	8.04	182.24	15.09
4	187.25	8.04	187.05	11.61	182.41	8.11	182.90	11.58
5	187.33	8.04	187.11	11.68	180.99	7.94	181.09	11.51
6	187.64	8.06	187.64	11.69	181.18	7.96	181.29	11.43
7	187.59	8.06	187.59	11.68	180.88	7.93	180.98	11.41
8	187.63	8.06	187.63	11.70	180.65	7.90	180.67	11.32
9	187.60	8.06	187.60	11.69	180.49	7.90	180.52	11.33
10	188.46	8.11	188.47	12.88	179.76	7.84	179.76	12.25
11	N.A.	N.A.	N.A.	N.A.	177.45	7.69	177.77	289.32
12	N.A.	N.A.	N.A.	N.A.	180.39	7.88	180.41	11.31
13	N.A.	N.A.	N.A.	N.A.	182.41	8.15	183.08	11.66
14	N.A.	N.A.	N.A.	N.A.	180.21	7.87	180.22	11.31
15 ^b	188.82	8.13	188.73	11.83	180.08	7.86	179.86	11.28

390 ^a no weighting, ^b ln-ln transformation

391

392 Ignoring heteroscedasticity resulted in estimates of mean AGB per hectare that were slightly
 393 different compared to estimates obtained from models calibrated with effective weighting of
 394 observations (Table 4). The differences were larger for Eq. (2) (models based on D), as great as 3.7%;
 395 therefore, when including H as a predictor variable, the negative effect of ignoring heteroscedasticity
 396 on mean AGB per hectare was reduced (differences less than 2.2%). Nevertheless, differences in
 397 estimates of mean AGB per hectare between model forms were greater than between weighting

398 procedures. Models based on D only, regardless of the weighting procedure, produced greater
399 estimates of mean AGB per hectare than did models based on both D and H (Table 4).

400 The weighting procedures that were effective in accommodating heteroscedasticity (p-values
401 larger than 0.05, Fig. 3) produced more consistent large-area estimates (mean AGB per hectare and
402 SE, Table 4). For example, for models based on D and H to predict AGB, although the largest
403 difference in mean AGB per hectare between any two weighting procedures was 5.6 Mg ha⁻¹ (i.e.,
404 weighting procedures 11 and 13, Table 4), the largest difference between any two effective weighting
405 procedures (p > 0.05, see Fig. 3) was 1.1 Mg ha⁻¹ (i.e., procedures 6 and 14, Table 4). Similar results
406 were observed for models based on D only (Table 4).

407 The estimates of uncertainty were also affected by the weighting procedure. For models based
408 on D only, ignoring heteroscedasticity resulted in a slight underestimation of SEs (compared to
409 uncertainty estimates from models that used weighting procedures effective in accommodating
410 heteroscedasticity), whereas for models based on both D and H, we observed an opposite effect, a
411 slight overestimation of uncertainty (Table 4). There were two weighting procedures (procedures 3
412 and 11, Table 2) that produced substantially overestimated uncertainty, suggesting that due care is
413 necessary when using fixed-parameter functions to model the standard deviation of heteroscedastic
414 residuals within the Monte Carlo error propagation procedure (see step 3b, section 2.3.2).

415

416 **3.3. The effects of allometric biomass model prediction uncertainty**

417 We compared the estimates of mean biomass per hectare and of uncertainty when both
418 including and excluding model prediction uncertainty for purposes of assessing the effects of this
419 source of uncertainty. As expected, the estimates of mean AGB per hectare were similar, especially
420 for weighting procedures that were effective in accommodating heteroscedasticity. Differences as
421 great as 1.2% were observed for models ignoring heteroscedasticity or using an ineffective weighting
422 procedure, and as great as 0.1% for models that used effective weighting procedures (Table 4).

423

424 Relative to the uncertainty that was due to sampling variability alone (SE, Eq. 11),
425 incorporating the model prediction uncertainty (SE, Eq. 17) resulted in substantial increase of SEs.

426 For the most effective weighting procedures ($p > 0.05$, see Fig. 3), when model prediction uncertainty
427 was included, the SE increased by 44.4% to 58.7% for models based on D-only and by 43.6% to
428 44.9% for models based on both D and H (Table 4). Therefore, the effects of allometric model
429 prediction uncertainty were less when both D and H were used to predict the AGB, because addition
430 of H as predictor variable resulted in a reduction of residual standard error of the model. Nevertheless,
431 for weighting procedures 3 and 11, the differences were substantial (as great as 3661%), given the
432 large overestimation of uncertainty shown earlier.

433 4. Discussion

434 We examined weighting approaches for power-law nonlinear allometric biomass models whose
435 prediction residuals exhibit heteroscedasticity. The results showed that some weighting procedures
436 were more effective in accommodating heteroscedasticity than others. In general, the weighting
437 procedures based on fixed parameter functions such as D^{-1} , D^{-2} , D^{-4} or $(D^2H)^{-2}$ were less effective
438 compared to specifically tailored functions (e.g., $D^{-\lambda}$, $\widehat{AGB}^{-\lambda}$). In fact, these fixed parameter
439 functions did not produce any p-value larger than 0.05 which, under the Breusch-Pagan test, means
440 effective compensation for heteroscedasticity (see Table 3) for any of the datasets. In addition, some
441 of the fixed parameter functions (e.g., D^{-4} and $(D^2H)^{-2}$) produced serious overestimation of
442 uncertainty. Therefore, we recommend avoiding using fixed parameter functions for weighting the
443 observations in allometric biomass models.

444 Because heteroscedasticity is evaluated against all predictor variables used in the model, it
445 was expected that for single predictor models the heteroscedasticity will be accommodated more
446 easily compared to models that have two or more predictor variables. For example, in our analysis,
447 given the number of datasets and number of weighting procedures, for models based on D only,
448 heteroscedasticity was adequately accommodated for 33 of 77 cases (Table 3 and Fig. 3), which
449 represents a ratio of 43%. By comparison, for models based on D and H, the heteroscedasticity was
450 adequately accommodated for only 12 out of 105 cases (Table 3 and Fig. 3), which indicates a much
451 smaller rate of just 11%. Modelling heteroscedasticity is challenging because variance can hardly be
452 approximated at the level of individual observations directly, without a grouping of the residuals first.
453 The data are recommended to be first ordered with respect to the model predictor variable in case of a
454 model with only a single predictor variable (which often was D or \widehat{AGB}). The procedure is more
455 complex when two predictor variables are used concomitantly to predict the heteroscedastic variance.
456 We used, however, four procedures that involved both D and H to predict the heteroscedastic
457 variance, of which only one approach was effective. Weighting procedure 14 was effective in five of
458 seven datasets, which is substantial, given the more complex nature of heteroscedasticity in models
459 with two predictors. Nevertheless, because using two or more predictor variables increases the

460 complexity of the heteroscedasticity models, using just the most significant predictor variable (e.g., D
461 or \widehat{AGB} as predictors of heteroscedasticity) should be preferred.

462 Both D and \widehat{AGB} can be used as predictors of heteroscedastic variance. Weighting procedures
463 6 and 8 are similar to procedures 7 and 9, respectively, except procedures 6 and 7 use D to predict
464 heteroscedastic variance, whereas procedures 8 and 9 use \widehat{AGB} . Comparable effectiveness of
465 weighting functions based on D and \widehat{AGB} in compensating for heteroscedasticity was observed with
466 the functions based on D being effective in 16 of 28 cases and functions based on \widehat{AGB} in 15 of 28
467 cases (Table 3 and Fig. 3). Therefore, either D or \widehat{AGB} can be used as predictor of heteroscedastic
468 variance with good results.

469 Modelling heteroscedasticity in two stages (modelling the heteroscedasticity resulted from a
470 weighted nonlinear model, as in procedures 7 and 9) produced weights that were more effective in
471 compensating for heteroscedasticity. Procedures 7 and 9 that used two modelling stages were 100%
472 effective for single predictor models (Table 3). The reason two stage modelling was more effective
473 was because the residuals that are modelled should be as similar as possible to those of the weighted
474 model. The residuals resulting from an unweighted nonlinear model can be sometimes slightly
475 different than those resulted from a weighted nonlinear model and, therefore, the group variance is
476 affected, thereby further affecting the parameter estimates for the heteroscedasticity model. Therefore,
477 we recommend using two modelling stages of heteroscedasticity, whenever a single stage modelling
478 is ineffective. Furthermore, it has been shown that weighted power-law nonlinear regression and
479 logarithmic transformation produce similar estimates of model parameters (Dutcă et al., 2019). As a
480 result, logarithmic transformation can be used as a first stage approximation, as it was used in
481 procedure 14, which had the greatest effectiveness (i.e., accommodating heteroscedasticity for five of
482 seven datasets, see Table 3 and Fig. 3) among models based on Eq. (3).

483 Logarithmic transformation has long been promoted as the standard way to fit allometric
484 models (Chave et al., 2014; Huxley, 1932; Kerkhoff and Enquist, 2009). Ln-ln transformation,
485 besides linearization of the power-law nonlinear model can also possibly serve as a way to
486 accommodate heteroscedasticity. In our application, the residuals became homoscedastic for three of

487 seven datasets in the case of single predictor models, whereas none of the models based on D and H
488 showed homoscedastic residuals as a result of transformation. However, the logarithmic
489 transformation, although failing to effectively accommodate heteroscedasticity (Fig. 3, procedure 15),
490 produced AGB estimates and SEs that were very similar to those resulting from weighting procedures
491 that satisfactorily accommodated heteroscedasticity (Table 4). As a result, ln-ln transformation can be
492 preferred to other ineffective weighting procedures (Table 3). Nevertheless, we recommend testing
493 the heteroscedasticity of residuals on ln-ln scale before selecting the ln-ln transformation as the
494 method to fit the models.

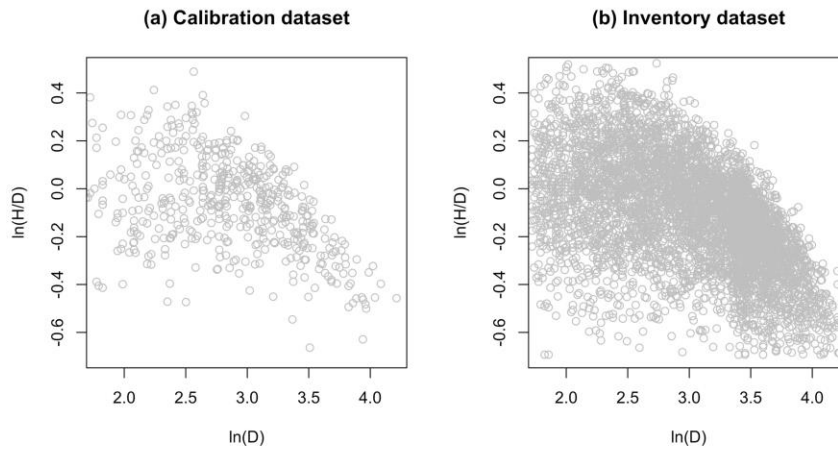
495 For weighting procedures that used grouping, the size of the groups when modelling the
496 heteroscedastic variance was an important parameter. We set up the group size to 25, because it was a
497 good compromise: it was large enough so that the group variances can be calculated in good
498 conditions, and small enough to catch most irregularities within the pattern of heteroscedastic
499 variance across the predictor range. However, the group size can be modified by the user to find an
500 accurate pattern of heteroscedasticity for each biomass model. Another important point is that when
501 sample size is small the grouping approach becomes challenging, to the point that if the group sample
502 size is very small, the grouping approach becomes irrelevant. In these conditions logarithmic
503 transformation remains a good compromise that can be used to fit the models.

504 The model form used to predict the heteroscedastic variance is also important. Our results
505 confirmed that, in general, heteroscedastic variance was well approximated by a power function of the
506 predictor variable (e.g., D or \widehat{AGB}). For some of the weighting procedures we employed the ln-ln
507 transformation instead of nonlinear fitting (see step (vi) of procedures 6 – 9, Table 2) for two reasons:
508 first, the user can easily check the linear fit by graphing the variables, and second, ln-ln
509 transformation may deal with potential presence of heteroscedasticity within the heteroscedasticity
510 model. Nevertheless, for weighting procedures 6 – 9 (Table 2) we performed a parallel analysis, using
511 nonlinear models instead of ln-ln transformation approach. When using ln-ln transformation, the mean
512 AGB per hectare varied between 180.49 Mg ha⁻¹ and 181.29 Mg ha⁻¹ (for weighting procedures 6 – 9,
513 Table 4). Using the nonlinear approach instead of ln-ln transformation, the estimates of mean AGB
514 per hectare were between 175.38 Mg ha⁻¹ and 181.71 Mg ha⁻¹. The estimates of uncertainty were less

515 affected. Therefore, using ln-ln transformation to model heteroscedasticity gives more consistent
516 estimates, this being the reason we recommend using the ln-ln transformation approach.

517 This general pattern of heteroscedasticity that is often described by a power function explains
518 why logarithmic transformation sometimes produces homoscedastic residuals in allometric models.
519 However, for weighting procedures that used two predictor variables to predict the heteroscedastic
520 variance (e.g., procedure 14) we observed for some datasets a nonlinear relationship on ln-ln scale,
521 between H and the group variance. Consequently, the relationship between heteroscedastic variance
522 and the predictor variables D and H was not well described by a power function. This was observed
523 for Datasets 6 and 7, for which procedure 14 was not effective in accommodating heteroscedasticity.
524 In such cases, more complex functions for predicting heteroscedastic variance may be investigated.

525 Our results showed a larger difference in estimates of mean AGB per hectare between model
526 forms (Eq. 2 vs. Eq. 3) than between weighting approaches within each model form. This difference
527 could be attributed to two different causes: (i) the effect of including H in allometric models, being
528 shown that addition of H in allometric models would improve the accuracy of AGB prediction,
529 compared to models based on D only (Dutcă, 2019; Dutcă et al., 2020) and (ii) model
530 misspecification as shown in Fig. (3). The models based on D only showed a nonlinear trend in the
531 weighted residuals that disappeared once H was added as predictor variable. This nonlinear trend in
532 the weighted residuals for models based on D only was likely caused by the relationship between D
533 and H, which is reflected by the H-D ratio. Small trees, usually growing in denser stands, with
534 stronger tree competition, exhibit a larger H-D ratio, compared to large trees (Vospersnik et al., 2010).
535 However, some of the small trees (i.e., small D) within our calibration dataset showed a comparable
536 H-D ratio to that of large trees (Fig. 4, a). Moreover, it is to be expected that for trees of similar D, a
537 smaller H-D ratio will result in a smaller observed AGB. Therefore, the nonlinear trend in the
538 residuals of models based on D (Fig. 3) was likely caused by a smaller-than-expected H for small
539 trees, reflected in the nonlinear trend of relationship between D and H-D ratio (presented in ln-ln
540 scale, see Fig. 4, a). A similar nonlinear trend was observed for the inventory dataset (Fig. 4, b),
541 confirming the good agreement between the calibration dataset and inventory dataset.



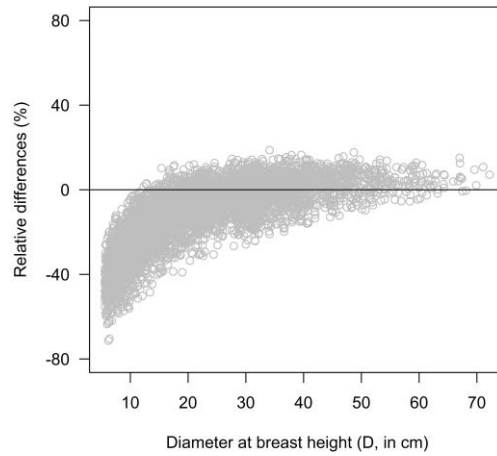
542

543 **Fig. 4.** The relationship between D and H-D ratio, in ln-ln scale, for the calibration dataset (a) and the inventory dataset (b).

544

545 The differences in estimates of mean AGB per hectare between different weighting
 546 approaches were generally small to moderate. For example, using both D and H to predict tree AGB
 547 (Eq. 3), the estimates of mean AGB per hectare were 181.50 Mg ha⁻¹ when ignoring
 548 heteroscedasticity (approach 0, Table 4) and 181.29 Mg ha⁻¹ for weighting approach 6 which,
 549 according to the p-value presented in Fig. 3, can be considered the most effective weighting approach
 550 when using Eq. 3. These results suggest a confirmation that ordinary least squares estimators of model
 551 parameters are unbiased in the presence of heteroscedasticity (Hayes and Cai, 2007; White, 1980).
 552 However, Mascaro et al. (2011) showed that ignoring heteroscedasticity may result in systematic
 553 errors in AGB predictions for small trees and, consequently, for plots containing small trees. To
 554 investigate this premise, for every tree in the inventory sample (section 2.1.2) we calculated the
 555 individual tree prediction differences between the unweighted nonlinear model and model using the
 556 weighting approach 6. These differences were then divided by the means of individual tree
 557 predictions (two predictions for each tree), to obtain the relative differences of individual tree
 558 predictions, as in Bland-Altman plots (Bland and Altman, 1986). In Fig. 5 can be observed that, for
 559 small trees, ignoring the heteroscedasticity resulted in underestimation of individual tree predictions
 560 as great as 71%, confirming the results of Mascaro et al. (2011). Nevertheless, despite these large
 561 relative differences for small trees, the estimates of mean AGB per hectare were barely different (i.e.,
 562 181.50 vs. 181.29 Mg ha⁻¹). We suspect that was because the differences in small trees, although

563 important when judged as relative differences, are negligible in terms of absolute values when
564 compared to estimates of the large trees.



565

566 **Fig. 5.** The relative differences in individual tree predictions when ignoring heteroscedasticity. Note: The relative differences
567 were calculated for each individual tree in the inventory dataset as: $(\widehat{AGB0}_i - \widehat{AGB1}_i) / (\frac{\widehat{AGB0}_i + \widehat{AGB1}_i}{2}) \cdot 100$, where $\widehat{AGB0}_i$ is
568 the predicted AGB of i^{th} tree in the inventory dataset based on unweighted nonlinear model (Eq. 3); $\widehat{AGB1}_i$ is the predicted
569 AGB of i^{th} tree in the inventory dataset, based on Eq. (3) with the weighting approach 6.

570

571 For models based on D and H, the coefficient of variation (i.e., SE relative to estimated mean
572 AGB per hectare) was approximately 6.3% when including model prediction uncertainty and
573 approximately 4.4% when ignoring model prediction uncertainty for models that used an effective
574 weighting procedure. Smaller ratios, of approximately 2.6% and 1.9% were reported by McRoberts
575 and Westfall (2014) and McRoberts et al. (2015), but involving a much larger number of plots
576 compared to our study (1074 and respectively 2178 plots, compared to 243 plots used in this study). A
577 comparable ratio of 5.0% was reported by Duncanson et al. (2017) based on 179 sample plots. The
578 uncertainty due to allometric model prediction was not negligible, as has been reported for some
579 studies (Breidenbach et al., 2014; McRoberts et al., 2016, 2015). For this study, this component of
580 uncertainty contributed to an approximate 45% increase in SEs and, therefore, we recommend that it
581 should at least be considered whenever using allometric biomass models.

582 **5. Conclusions**

583 The conclusions of this study can be summarized as follows:

- 584 (i) We tested several procedures for weighting of observations to accommodate
585 heteroscedasticity in allometric biomass models. Some weighting procedures were more
586 effective than others in accommodating heteroscedasticity. For single predictor models,
587 heteroscedasticity was more effectively accommodated than for models based on D and H.
588 For models based on D only, weighting procedures 7 and 9 were 100% effective in
589 accommodating heteroscedasticity; for models based on D and H, procedure 14 was the most
590 effective.
- 591 (ii) Failing to effectively accommodate heteroscedasticity resulted in small-to-moderate
592 differences of estimates of mean AGB per hectare and of standard errors.
- 593 (iii) Including H as predictor variable in allometric biomass models greatly improved the AGB
594 prediction. The estimates of mean AGB per hectare and of standard errors were more
595 seriously affected by omitting H as a predictor of AGB (models based on D and H versus
596 models based on D only), than by the weighting approach. Therefore, we highly recommend
597 including H as predictor variable in allometric biomass models.
- 598 (iv) The standard errors of the estimated mean AGB per hectare increased by 44-59% when model
599 prediction uncertainty was included, therefore, we recommend incorporating model
600 prediction uncertainty in the total uncertainty estimate.
- 601 (v) We highly recommend testing the efficiency of the weighting procedure by using the adapted
602 Breusch-Pagan test proposed here.

603

604

605 **CRedit author statement:**

606 Ioan Ducea: Conceptualization, Methodology, Formal analysis, Writing – original draft; Ronald E.

607 McRoberts: Conceptualization, Methodology, Writing – reviewing and editing; Erik Næsset: Writing

608 – reviewing and editing; Viorel N.B. Blujdea: Writing – reviewing and editing.

609

610

611 **Abbreviations:**

612 AGB – aboveground biomass; D – diameter at breast height (1.3 m from the ground); H – tree height;

613 SE – standard error.

614

615

616 **Funding:** This work was supported by a grant of the Romanian Ministry of Education and Research,

617 CNCS—UEFISCDI, within PNCDI III [project number PN-III-P1-1.1-TE-2019-1744,

618 BIOPREDICT]; and by ERA-NET FACCE ERA-GAS and with national support from Romanian

619 National Authority for Scientific Research and Innovation, CCCDI – UEFISCDI [grant number

620 82/2017, FORCLIMIT project]. FACCE ERA-GAS has received funding from the European Union’s

621 Horizon 2020 research and innovation programme [grant agreement 696356].

622

623

624 **References**

625

626 Asrat, Z., Eid, T., Gobakken, T., Negash, M., 2020. Modelling and quantifying tree biometric
627 properties of dry Afromontane forests of south-central Ethiopia. *Trees - Struct. Funct.* 34, 1411–
628 1426. doi:10.1007/s00468-020-02012-8

629 Balboa-Murias, M.Á., Rodríguez-Soalleiro, R., Merino, A., Álvarez-González, J.G., 2006. Temporal
630 variations and distribution of carbon stocks in aboveground biomass of radiata pine and
631 maritime pine pure stands under different silvicultural alternatives. *For. Ecol. Manage.* 237, 29–
632 38. doi:10.1016/J.FORECO.2006.09.024

633 Baskerville, G.L., 1972. Use of Logarithmic Regression in the Estimation of Plant Biomass. *Can. J.*
634 *For. Res.* 2, 49–53. doi:10.1139/x72-009

635 Bland, J.M., Altman, D., 1986. Statistical methods for assessing agreement between two methods of
636 clinical measurement. *Lancet* 327, 307–310. doi:doi.org/10.1016/S0140-6736(86)90837-8

637 Bonan, G.B., 2008. Forests and climate change: forcings, feedbacks, and the climate benefits of
638 forests. *Science* 320, 1444–9. doi:10.1126/science.1155121

639 Breidenbach, J., Anton-Fernandez, C., Petersson, H., Mcroberts, R.E., Astrup, R., 2014. Quantifying
640 the model-related variability of biomass stock and change estimates in the Norwegian national
641 forest inventory. *For. Sci.* 60, 25–33. doi:10.5849/forsci.12-137

642 Breusch, T.S., Pagan, A.R., 1979. A simple test for heteroscedasticity and random coefficient
643 variation. *Econometrica* 47, 1287–1294. doi:10.2307/1911963

644 Canadell, J.G., Raupach, M.R., 2008. Managing forests for climate change mitigation. *Science* 320,
645 1456–7. doi:10.1126/science.1155458

646 Chave, J., Andalo, C., Brown, S., Cairns, M.A., Chambers, J.Q., Eamus, D., Fölster, H., Fromard, F.,
647 Higuchi, N., Kira, T., Lescure, J.P., Nelson, B.W., Ogawa, H., Puig, H., Riéra, B., Yamakura,
648 T., 2005. Tree allometry and improved estimation of carbon stocks and balance in tropical
649 forests. *Oecologia* 145, 87–99. doi:10.1007/s00442-005-0100-x

650 Chave, J., Réjou-Méchain, M., Búrquez, A., Chidumayo, E., Colgan, M.S., Delitti, W.B.C., Duque,
651 A., Eid, T., Fearnside, P.M., Goodman, R.C., Henry, M., Martínez-Yrizar, A., Mugasha, W.A.,

652 Muller-Landau, H.C., Mencuccini, M., Nelson, B.W., Ngomanda, A., Nogueira, E.M., Ortiz-
653 Malavassi, E., Péliissier, R., Ploton, P., Ryan, C.M., Saldarriaga, J.G., Vieilledent, G., 2014.
654 Improved allometric models to estimate the aboveground biomass of tropical trees. *Glob. Chang.*
655 *Biol.* 20, 3177–3190. doi:10.1111/gcb.12629

656 Cochran, W., 1977. *Sampling Techniques*, Third edit. ed. John Wiley & Sons, New York.

657 Condés, S., McRoberts, R.E., 2017. Updating national forest inventory estimates of growing stock
658 volume using hybrid inference. *For. Ecol. Manage.* 400, 48–57.
659 doi:10.1016/J.FORECO.2017.04.046

660 Corona, P., Fattorini, L., Franceschi, S., Scrinzi, G., Torresan, C., 2014. Estimation of standing wood
661 volume in forest compartments by exploiting airborne laser scanning information: Model-based,
662 Design-based, And hybrid perspectives. *Can. J. For. Res.* 44, 1303–1311. doi:10.1139/cjfr-2014-
663 0203

664 Cunia, T., 1964. Weighted Least Squares Method and Construction of Volume Tables. *For. Sci.* 10,
665 180–191. doi:10.1093/forestscience/10.2.180

666 Duncanson, L., Huang, W., Johnson, K., Swatantran, A., McRoberts, R.E., Dubayah, R., 2017.
667 Implications of allometric model selection for county-level biomass mapping. *Carbon Balance*
668 *Manag.* 12, 18. doi:10.1186/s13021-017-0086-9

669 Dutcă, I., 2019. The Variation Driven by Differences between Species and between Sites in
670 Allometric Biomass Models. *Forests* 10, 976. doi:10.3390/f10110976

671 Dutcă, I., 2018. Biomass data for young, planted Norway spruce trees in Eastern Carpathians of
672 Romania. *Data Br.* 19, 2384–2392. doi:10.1016/j.dib.2018.07.033

673 Dutcă, I., Mather, R., Blujdea, V.N.B., Ioraş, F., Olari, M., Abrudan, I.V., 2018. Site-effects on
674 biomass allometric models for early growth plantations of Norway spruce (*Picea abies* (L.)
675 Karst.). *Biomass and Bioenergy* 116, 8–17. doi:10.1016/j.biombioe.2018.05.013

676 Dutcă, I., McRoberts, R.E., Næsset, E., Blujdea, V.N.B., 2019. A practical measure for determining if
677 diameter (D) and height (H) should be combined into D2H in allometric biomass models. *For.*
678 *An Int. J. For. Res.* 92, 627–634. doi:10.1093/forestry/cpz041

679 Dutcă, I., Zianis, D., Petrişan, I.C., Bragă, C.I., Ştefan, G., Yuste, J.C., Petrişan, A.M., 2020.

680 Allometric biomass models for european beech and silver fir: Testing approaches to minimize
681 the demand for site-specific biomass observations. *Forests* 11. doi:10.3390/f11111136

682 Falster, D.S., Duursma, R.A., Ishihara, M.I., Barneche, D.R., FitzJohn, R.G., Vårhammar, A., Aiba,
683 M., Ando, M., Anten, N., Aspinwall, M.J., Baltzer, J.L., Baraloto, C., Battaglia, M., Battles, J.J.,
684 Bond-Lamberty, B., van Breugel, M., Camac, J., Claveau, Y., Coll, L., Dannoura, M.,
685 Delagrangé, S., Domec, J.-C., Fatemi, F., Feng, W., Gargaglione, V., Goto, Y., Hagihara, A.,
686 Hall, J.S., Hamilton, S., Harja, D., Hiura, T., Holdaway, R., Hutley, L.S., Ichie, T., Jokela, E.J.,
687 Kantola, A., Kelly, J.W.G., Kenzo, T., King, D., Kloeppe, B.D., Kohyama, T., Komiyama, A.,
688 Laclau, J.-P., Lusk, C.H., Maguire, D.A., le Maire, G., Mäkelä, A., Markesteijn, L., Marshall, J.,
689 McCulloh, K., Miyata, I., Mokany, K., Mori, S., Myster, R.W., Nagano, M., Naidu, S.L.,
690 Nouvellon, Y., O'Grady, A.P., O'Hara, K.L., Ohtsuka, T., Osada, N., Osunkoya, O.O., Peri,
691 P.L., Petritan, A.M., Poorter, L., Portsmouth, A., Potvin, C., Ransijn, J., Reid, D., Ribeiro, S.C.,
692 Roberts, S.D., Rodríguez, R., Saldaña-Acosta, A., Santa-Regina, I., Sasa, K., Selaya, N.G.,
693 Sillett, S.C., Sterck, F., Takagi, K., Tange, T., Tanouchi, H., Tissue, D., Umehara, T., Utsugi,
694 H., Vadeboncoeur, M.A., Valladares, F., Vanninen, P., Wang, J.R., Wenk, E., Williams, R., de
695 Aquino Ximenes, F., Yamaba, A., Yamada, T., Yamakura, T., Yanai, R.D., York, R.A., 2015.
696 BAAD: a Biomass And Allometry Database for woody plants. *Ecology* 96, 1445–1445.
697 doi:10.1890/14-1889.1

698 Forrester, D.I., Tachauer, I.H.H., Annighoefer, P., Barbeito, I., Pretzsch, H., Ruiz-Peinado, R., Stark,
699 H., Vacchiano, G., Zlatanov, T., Chakraborty, T., Saha, S., Sileshi, G.W., 2017. Generalized
700 biomass and leaf area allometric equations for European tree species incorporating stand
701 structure, tree age and climate. *For. Ecol. Manage.* 396, 160–175.
702 doi:10.1016/j.foreco.2017.04.011

703 Goldberger, A.S., 1968. The Interpretation and Estimation of Cobb-Douglas Functions. *Econometrica*
704 36, 464–472. doi:10.2307/1909517

705 Grassi, G., House, J., Dentener, F., Federici, S., den Elzen, M., Penman, J., 2017. The key role of
706 forests in meeting climate targets requires science for credible mitigation. *Nat. Clim. Chang.* 7,
707 220–226. doi:10.1038/nclimate3227

708 Harvey, A.C., 1976. Estimating Regression Models with Multiplicative Heteroscedasticity.
709 *Econometrica* 44, 461–465. doi:10.2307/1913974

710 Hayes, A.F., Cai, L., 2007. Using heteroskedasticity-consistent standard error estimators in OLS
711 regression: An introduction and software implementation. *Behav. Res. Methods* 39, 709–722.

712 Huff, S., Poudel, K.P., Ritchie, M., Temesgen, H., 2018. Quantifying aboveground biomass for
713 common shrubs in northeastern California using nonlinear mixed effect models. *For. Ecol.
714 Manage.* 424, 154–163. doi:10.1016/J.FORECO.2018.04.043

715 Huxley, S.J., 1932. *Problems of Relative Growth*, 1st ed. The Dial Press, New York.
716 doi:10.1038/129775a0

717 Huy, B., Thanh, G., Poudel, K., Temesgen, H., 2019. Individual Plant Allometric Equations for
718 Estimating Aboveground Biomass and Its Components for a Common Bamboo Species
719 (*Bambusa procera* A. Chev. and A. Camus) in Tropical Forests. *Forests* 10, 316.
720 doi:10.3390/f10040316

721 Jacobs, M.W., Monteith, D.B., 1981. Feasibility of Developing Regional Weight Tables. *J. For.* 79,
722 676–677. doi:10.1093/jof/79.10.676

723 Kerkhoff, A.J., Enquist, B.J., 2009. Multiplicative by nature: Why logarithmic transformation is
724 necessary in allometry. *J. Theor. Biol.* 257, 519–521. doi:10.1016/j.jtbi.2008.12.026

725 Kralicek, K., Huy, B., Poudel, K.P., Temesgen, H., Salas, C., 2017. Simultaneous estimation of
726 above-and below-ground biomass in tropical forests of Viet Nam principle System of equations
727 Dipterocarp forest Evergreen broadleaf forest Tropical forest. *For. Ecol. Manage.* 390, 147–156.
728 doi:10.1016/j.foreco.2017.01.030

729 Luo, Y., Wang, X., Ouyang, Z., Lu, F., Feng, L., Tao, J., 2020. A review of biomass equations for
730 China’s tree species. *Earth Syst. Sci. Data* 12, 21–40. doi:10.5194/essd-12-21-2020

731 Marin, G., Strimbu, V.C., Abrudan, I. V., Strimbu, B.M., 2020. Regional variability of the Romanian
732 main tree species growth using national forest inventory increment cores. *Forests* 11, 1–18.
733 doi:10.3390/F11040409

734 Mascaro, J., Litton, C.M., Hughes, R.F., Uowolo, A., Schnitzer, S.A., 2011. Minimizing Bias in
735 Biomass Allometry: Model Selection and Log-Transformation of Data. *Biotropica* 43, 649–653.

736 doi:10.1111/j.1744-7429.2011.00798.x

737 McRoberts, R.E., Chen, Q., Domke, G.M., Ståhl, G., Saarela, S., Westfall, J.A., 2016. Hybrid
738 estimators for mean aboveground carbon per unit area. *For. Ecol. Manage.* 378, 44–56.
739 doi:10.1016/J.FORECO.2016.07.007

740 McRoberts, R.E., Moser, P., Zimmermann Oliveira, L., Vibrans, A.C., 2015. A general method for
741 assessing the effects of uncertainty in individual-tree volume model predictions on large-area
742 volume estimates with a subtropical forest illustration. *Can. J. For. Res.* 45, 44–51.
743 doi:10.1139/cjfr-2014-0266

744 McRoberts, R.E., Næsset, E., Saatchi, S., Liknes, G.C., Walters, B.F., Chen, Q., 2019. Local
745 validation of global biomass maps. *Int. J. Appl. Earth Obs. Geoinf.* 83, 101931.
746 doi:10.1016/j.jag.2019.101931

747 McRoberts, R.E., Westfall, J.A., 2014. Effects of Uncertainty in Model Predictions of Individual Tree
748 Volume on Large Area Volume Estimates. *For. Sci.* 60, 34–42. doi:10.5849/forsci.12-141

749 Meng, C.H., Tsai, W.Y., 1986. Selection of weights for a weighted regression of tree volume. *Can. J.*
750 *For. Res.* 16, 671–673. doi:10.1139/x86-118

751 Packard, G.C., 2014. On the use of log-transformation versus nonlinear regression for analyzing
752 biological power laws. *Biol. J. Linn. Soc.* 113, 1167–1178. doi:10.1111/bij.12396

753 Packard, G.C., Boardman, T.J., 2008. Model selection and logarithmic transformation in allometric
754 analysis. *Physiol. Biochem. Zool.* 81, 496–507. doi:10.1086/589110

755 Pan, Y., Birdsey, R.A., Fang, J., Houghton, R., Kauppi, P.E., Kurz, W.A., Phillips, O.L., Shvidenko,
756 A., Lewis, S.L., Canadell, J.G., Ciais, P., Jackson, R.B., Pacala, S.W., McGuire, A.D., Piao, S.,
757 Rautiainen, A., Sitch, S., Hayes, D., 2011. A large and persistent carbon sink in the world's
758 forests. *Science* 333, 988–93. doi:10.1126/science.1201609

759 Park, R.E., 1966. Estimation with heteroscedastic error terms. *Econometrica* 34, 888.

760 Parresol, B.R., 1993. Modeling multiplicative error variance - An example predicting tree diameter
761 from stump dimensions in baldcypress. *For. Sci.* 39, 670–679.
762 doi:10.1093/forestscience/39.4.670

763 Picard, N., Rutishauser, E., Ploton, P., Ngomanda, A., Henry, M., 2015. Should tree biomass

764 allometry be restricted to power models? *For. Ecol. Manage.* 353, 156–163.
765 doi:10.1016/j.foreco.2015.05.035

766 Picard, N., Saint-André, L., Henry, M., 2012. Manual for building tree volume and biomass allometric
767 equations: from field measurement to prediction. FAO and CIRAD, Rome, Italy, and
768 Montpellier, France.

769 R Core Team, 2017. R: A language and environment for statistical computing. R Foundation for
770 Statistical Computing, Vienna, Austria.

771 RStudio Team, 2016. RStudio: Integrated Development for R. RStudio, Inc., Boston, MA.

772 Rutishauser, E., Noor'an, F., Laumonier, Y., Halperin, J., Rufi'ie, Hergoualch, K., Verchot, L., 2013.
773 Generic allometric models including height best estimate forest biomass and carbon stocks in
774 Indonesia. *For. Ecol. Manage.* 307, 219–225. doi:10.1016/j.foreco.2013.07.013

775 Saint-André, L., M'Bou, A.T., Mabilia, A., Mouvondy, W., Jourdan, C., Roupsard, O., Deleporte, P.,
776 Hamel, O., Nouvellon, Y., 2005. Age-related equations for above- and below-ground biomass of
777 a Eucalyptus hybrid in Congo. *For. Ecol. Manage.* 205, 199–214.
778 doi:10.1016/j.foreco.2004.10.006

779 Särndal, C.-E., Swensson, B., Wretman, J., 1992. Model Assisted Survey Sampling. Springer Series
780 in Statistics, New York.

781 Schepaschenko, D., Shvidenko, A., Usoltsev, V., Lakyda, P., Luo, Y., Vasylyshyn, R., Lakyda, I.,
782 Myklush, Y., See, L., McCallum, I., Fritz, S., Kraxner, F., Obersteiner, M., 2017. A dataset of
783 forest biomass structure for Eurasia. *Sci. Data* 4, 170070. doi:10.1038/sdata.2017.70

784 Sprugel, D.G., 1983. Correcting for Bias in Log-Transformed Allometric Equations. *Ecology* 64,
785 209–210. doi:10.2307/1937343

786 Ståhl, G., Saarela, S., Schnell, S., Holm, S., Breidenbach, J., Healey, S.P., Patterson, P.L., Magnussen,
787 S., Næsset, E., McRoberts, R.E., Gregoire, T.G., 2016. Use of models in large-area forest
788 surveys: comparing model-assisted, model-based and hybrid estimation. *For. Ecosyst.* 3, 5.
789 doi:10.1186/s40663-016-0064-9

790 Ung, C.H., Lambert, M.C., Raulier, F., Guo, X.J., Bernier, P.Y., 2017. Biomass of trees sampled
791 across Canada as part of the Energy from the Forest Biomass (ENFOR) Program [WWW

792 Document]. doi:<https://doi.org/10.23687/fbad665e-8ac9-4635-9f84-e4fd53a6253c>

793 Venables, W.N. (William N.). (William N., Ripley, B.D., Venables, W.N. (William N.). (William
794 N., 2002. *Modern applied statistics with S*, 4th ed. Springer, New York.

795 Vieilledent, G., Vaudry, R., Andriamanohisoa, S.F.D., Rakotonarivo, O.S., Randrianasolo, H.Z.,
796 Razafindrabe, H.N., Bidaud Rakotoarivony, C., Ebeling, J., Rasamoelina, A.M., Rakotoarivony,
797 C.B., Ebeling, J., Rasamoelina, M., 2012. A universal approach to estimate biomass and carbon
798 stock in tropical forests using generic allometric models. *Ecol. Appl.* 22, 572–583.
799 doi:10.1890/11-0039.1

800 Vonderach, C., Kändler, G., Dormann, C.F., 2018. Consistent set of additive biomass functions for
801 eight tree species in Germany fit by nonlinear seemingly unrelated regression. *Ann. For. Sci.* 75,
802 49. doi:10.1007/s13595-018-0728-4

803 Vospernik, S., Monserud, R.A., Sterba, H., 2010. Do individual-tree growth models correctly
804 represent height:diameter ratios of Norway spruce and Scots pine? *For. Ecol. Manage.* 260,
805 1735–1753. doi:10.1016/j.foreco.2010.07.055

806 White, H., 1980. A heteroskedasticity-consistent covariance matrix estimator and a direct test for
807 heteroskedasticity. *Econometrica* 48, 817–838.

808 Williams, M.S., Gregoire, T.G., 1993. Estimating weights when fitting linear regression models for
809 tree volume. *Can. J. For. Res.* 23, 1725–1731. doi:10.1139/x93-216

810 Xiao, X., White, E.P., Hooten, M.B., Durham, S.L., 2011. On the use of log-transformation vs.
811 nonlinear regression for analyzing biological power laws. *Ecology* 92, 1887–1894.
812 doi:10.1890/11-0538.1

813 Zianis, D., Mencuccini, M., 2004. On simplifying allometric analyses of forest biomass. *For. Ecol.*
814 *Manage.* 187, 311–332. doi:10.1016/j.foreco.2003.07.007

815 Zianis, D., Muukkonen, P., Mäkipää, R., Mencuccini, M., 2005. Biomass and stem volume equations
816 for tree species in Europe. Finnish Society of Forest Science, Finnish Forest Research Institute.
817